Experimental and numerical study of the effect of vibration on airflow between can combustor liner and casing

Rami Y. Dahham[1,*], Dhirgham Alkhafaji[1], Hayder Al-Jelawy[2], Sattar J. Hadi[3]

1. Department of Mechanical Engineering, College of Engineering, University of Babylon, P.O.Box No 4 Hilla, Iraq

2. Faculty of Arts, Science and Technology, Department of Engineering, the University of Northampton, United Kingdom

3. Head of Operations Department at Al-Khairat Gas Turbine Power Station, Iraq

ramidahham@gmail.com

ABSTRACT. *The airflow in the can combustion generates significant instabilities. This interaction between the airflow and the combustor walls will induce vibration, which might result as strong fluctuations in the wall structure of the combustor. The present work is investigating the flow induced vibration, and four different locations have been selected to measure the velocity distribution, turbulent intensity, and static pressure recovery coefficient under forced vibration at three different frequencies (34, 48, 65 and 80 Hz) in the upper annulus of the Can Combustor. This phenomenon has been studied experimentally and numerically. The Computational Fluid Dynamics analysis was accomplished by utilizing the Shear-Stress Transport (SST) k-omega model to predict the flow velocity at the recirculation zone. The vibration testing equipment was designed and used to apply the excitation forces on the wall combustor. It has been explained that the reversed flow which causes eddies inside the recirculation region can be increased at higher frequencies. In addition to that, exciting the system with higher frequencies would increase the turbulence intensity causing a recirculation region enlargement. The Computational results were compared against the experimental results, and they show a very good agreement. On the other hand, the static pressure distribution has been decreased while increasing the frequency. It has been proved that the frequency values play an essential role to predict the system behavior.*

RÉSUMÉ. *Le flux d'air dans la combustion de cannettes génère des instabilités importantes. Cette interaction entre le flux d'air et les parois de chambre de combustion va induire des vibrations, ce qui pourrait entraîner que des fluctuations fortes dans la structure de paroi de la chambre de combustion. Le présent travail étudie les vibrations induites par le flux, et quatre endroits différents ont été sélectionnés pour mesurer la distribution de la vitesse, l'intensité de la turbulance, et le coefficient de récupération de pression statique sous vibration forcée à trois fréquences différentes (34, 48, 65 et 80 Hz) dans le anneau supérieur du brûleur de cannettes.*

Instrumentation, Mesure, Métrologie – n° 2/2018, 235-257

Ce phénomène a été étudié expérimentalement et informatiquement. L'analyse numérique de la dynamique des fluides a été réalisée en utilisant le modèle k-oméga de transport de contrainte de cisaillement (SST) pour prévoir la vitesse d'écoulement dans la zone de recirculation. L'équipement d'essai de vibration a été conçu et utilisé pour appliquer les forces d'excitation sur la chambre de combustion murale. Il a été expliqué que le flux inversé qui provoque des tourbillons à l'intérieur de la zone de recirculation peut être augmenté à des fréquences plus élevées. En plus de cela, l'excitation du système avec des fréquences plus élevées augmenterait l'intensité de la turbulence, ce qui provoquerait un élargissement de la région de recirculation. Les résultats informatiques ont été comparés aux résultats expérimentaux et montrent un très bon accord. D'autre part, la distribution de la pression statique a été réduite tout en augmentant la fréquence. Il a été prouvé que les valeurs de fréquence jouent un rôle essentiel dans la prédiction du comportement du système.

KEYWORDS: *annulus flow, can combustor, CFD Simulation, pitot - static tube, velocity profile, fluid-structure interface, forced vibration and flow-induced vibration.*

MOTS-CLÉS: *flux annulaire, brûleur de cannettes, simulation CFD, pitot - tube statique, profil de vitesse, interface de fluide-structure, vibration forcée et vibration induite par le flux.*

DOI:10.3166/I2M.17.235-257 © 2018 Lavoisier

1. Introduction

Generally, the rise of vibration levels in mechanical systems leads to an undesirable effect on the performance of this equipment. These vibrations might come from the rotating part of the system. One of these problems is the influence of vibration on the flow inside annulus for Can-Combustor for a gas turbine engine. The vibration which can be generated by the compressor and turbine is transferred through bearings to the combustor of the gas turbine engine. The manufacturing always supplies the allowance level of vibration which gives a normal performance of the engine. This study investigates the vibration effects on flow in the annulus of a Can Combustor supplied by Al-khairat power station/Iraq, manufactured by general electric company (GE). It was mentioned that at the Root Mean Square Amplitude (12.5 mm/s) RMS, the system's alarm will start warning and at (25 mm/s) RMS, the machine will stop causing an emergency shutdown. Moreover, this study investigates the airflow performance inside the annulus of the combustor with a range of waveform vibration (10-25 mm/s) RMS, figure 1 shows the control screen of the system called (HMI):

The Can Combustion burns a huge amount of fuel inside its chamber which is supplied by fuel nozzle sprayers, with enormous volumes of air supplied by the compressor. Generally, the combustor has four main components: diffuser, casing, liner, and annulus (Alqaraghuli *et al.*, 2014). This task must be accomplished with minimal pressure loss and maximum heat generated in the limited space available.

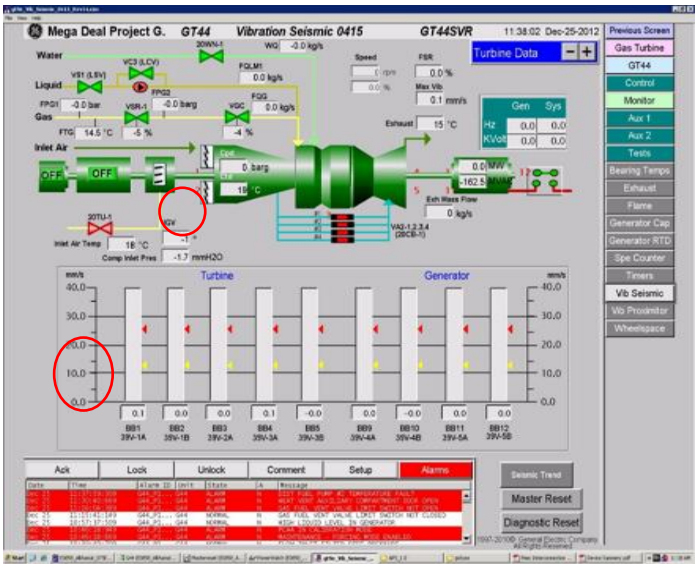

Figure 1. HMI screen

A wide range of studies have been published in this area. In their work, Hsieh *et al.* (2017) studied the eddy-produced vibration in the initial branch of a circular cylinder. However, Zhang *et al.* (2015) it considered examination of flow and blending attributes of supersonic mixing layer investigated by constrained vibration of cantilever. Their outcomes demonstrate that the difference the development of supersonic blending layer is different without vibration, the flow under forced vibration might show the characteristics of three-dimensionality. Zena and Hadi (2016) examined improvement of natural convection when applying the forced vibration to the corrugated surface, the result was the vibrational heat transfer coefficient increases with increased frequency of the surface. On the other hand, Poursaeidi *et al.* (2013) studied choking and assembly resonance problems, 3D models of the combustion chamber configuration and combustion flow were planned with finite element and estimate fluid dynamics behavior. They have compared the results of combustion chamber natural frequencies with combustion swirl frequency reveal that the chamber configuration is not under resonance. Huls *et al.*, (2007) studied how to reduce nitrogen oxides emissions from combustion systems, and a higher sensitivity to combustion variables, leads to an increased pressure levels in the combustor and generates the excitation from the surrounding structure which could start the fatigue propagation. Apparently, this will reduce the lifetime of the combustor. Elbaloshi, A. *et al.* (2014) have computationally investigated the three k-ε family turbulence models and k-ω family models. Shih *et al.* (2009) have studied characteristics of the can combustion process with a rotating casing for an advanced gas turbine. They found that when the rotational speed becomes high, the impact of the swirling flows outside the combustor can exceed the level in which the combustor can afford. Al-Shorafa"a

(2008) studied the effect of perpendicular vibration on heat transfer coefficient of horizontal cylinders. The conclusion was that the heat transfer ratio increases at high frequency. In their work, Rahim *et al.* (2012) investigate casing geometry influence on flow for Can Combustor. Their result showed that the velocity distribution is more stable for a diverging shape of the combustor. Wu *et al.* (2016) studied the effect of outlet layout on rotating flows in the combustor of gas turbine model experimentally and numerically. Kwark and Rao, (2012) observed thar at high Reynolds number, the turbulence intensity increases significantly.

2. Investigation of experimental setup

A real can combustor system has been used for this study which has been provided by the Al-Khairat Station (GTPP) in Iraq. This part has been connected to wind tunnel of subsonic flow, which has a square cross-sectional area. The vibration shaker has been designed to generate the proposed range of frequencies. The forced vibration was applied by the vibration shaker with different levels of frequencies (34, 48, 65 and 80 Hz) and amplitude value (0.0001 m). Accelerometers have been connected to a LabVIEW software through a sound and vibration device (USB-4431). The frequencies response has been calculated. The measurement locations were selected to be before and after the primary and secondary expansion area as well as before the dilution holes (X1=4cm, X2=20cm, X3=34, X4=60cm) respectively as shown in figure 6.

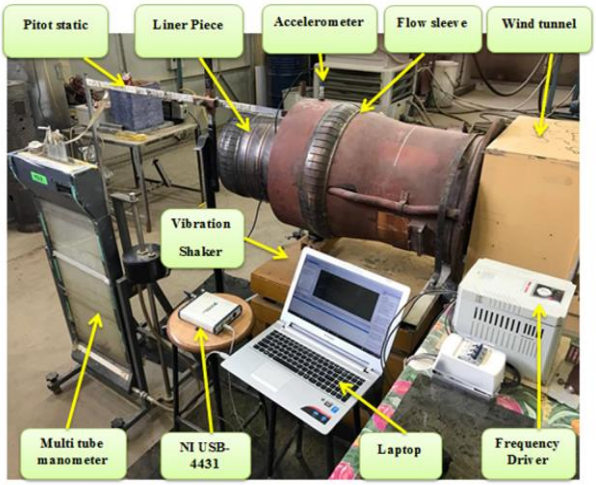

Figure 2. Experimental setup

In this research, a pitot-static tube has been used to calculate the pressure values as well as the pressure differences at different locations (upper and lower annulus) of the combustor. The velocity was also calculated at for locations at the upper and lower

annulus of can combustor where pressure difference was obtained at a selected point and applied Bernoulli equation as shown in figure1. The airflow was applied to the Combustor by the wind tunnel at atmospheric pressure. Figure 2 shows the experimental setup and figure 3 shows the schematic diagram of the test rig. The geometry of the Can-Annulus chamber consists cylindrical air casing diffuser with diameter of (42-52 cm) and its length is 73 cm. The internal liner diameter is 36 cm and its length is 100 cm.

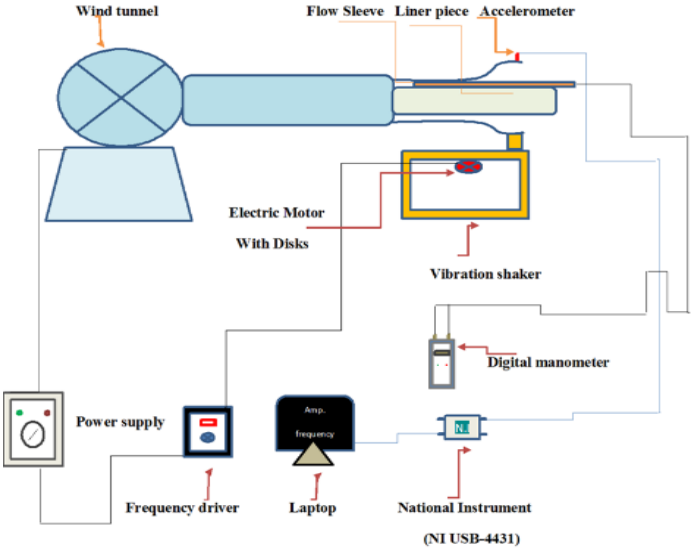

Figure 3. Schematic diagram

3. Vibration rig

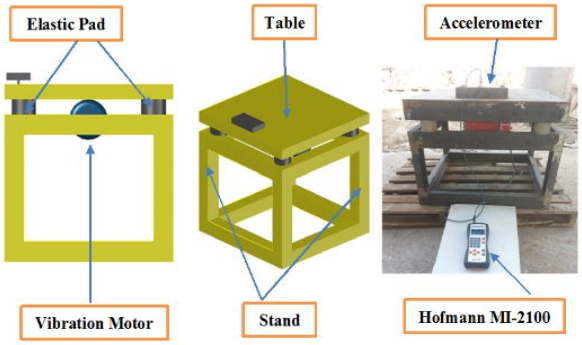

Figure 4. The Vibration test shaker

The vibration test equipment (the shaker) dimensions are 70*70*70 cm for each the length, width and height, respectively. The required vibration values were assumed to emulate the values in the Al-khairat power plant gas turbine engine, and these values are determined by using a vibration meter borrowed from the same power plant called (Hofmann MI 2100). The device consists of an electric motor with a capacity of 0.75 KW, speed is 2840 R.P.M, and it contains four non-concentric disks, which in turn generate vibration. The table on which the electric motor was based then manufactured, to transmit vibration values of the desired part (Can Combustor). The vibration control method has been considered by using a control device called (Frequency Driver), it controls electric motor speed; figure 4 explain the vibration test shaker.

4. Experimental procedure

This experimental study was performed according to the following procedures:

1. Setup all the hardware of the experimental test rig taking into consideration the safety conditions to ensure perfect and safe operation.

2. Setup the pressure rake on top of the annulus of the Can Combustor.

3. Connecting the system to the wind tunnel.

4. Taking measurements for upper annulus (first location, X=4 cm) and measure the pressures after five minutes to reach a steady state without vibration, then, the velocity distribution has been calculated, and the same procedure for the second, third and the fourth locations (X=20, 34 and 60 cm).

5. Switching the wind tunnel off.

6. Moving the rake pressure from the first station to the second station then run the wind tunnel again to measure the pressure.

8. Repeating step (5) for all proposed locations.

9. Repeating the same procedure above but with vibration effect.

5. Flow velocity calculation

To measure the velocity of incompressible fluid it used the Bernoulli's equation (Cengel *et al.*, 2008):

$$V = \sqrt{\frac{2(p_{total} - p_{static})}{\rho}} \quad (1)$$

6. Turbulence intensity

The turbulence intensity, *I*, defined as the ratio of the root-mean-square of the velocity fluctuations, to the mean flow velocity:

$$I = \frac{\acute{u}}{u_{avg}} = \frac{(\frac{2k}{3})^{\frac{1}{2}}}{u_{avg}} \quad (2)$$

7. Static pressure recovery coefficient C_p

The Static pressure recovery coefficient is defined as the difference in average static pressure between first and last station:

$$C_p = \frac{P_{s_2} - P_{s_1}}{P_{t_1} - P_{s_1}} \quad (3)$$

8. Air Properties and boundary conditions

The air is the fluid, which is used in this project, so the properties of air are taken at atmospheric pressure and temperature 300 K, as shown in table 1:

Table 1. Air Properties

Parameters	Units	Values
(ρ)	kg/m^3	1.1774
(Cp)	J/(kg .K)	1005.7
(k)	W/(m. K)	0.02624
Dynamic viscosity (μ)	kg/m. s	1.8462*10−5

9. Computational model

A commercial obtainable computational fluid dynamics (CFD) code "ANSYS-FLUENT 16.0" was used for the analysis. A combustion model was created from 2-D geometry using SolidWorks 2016 software as shown in figure 5. The CAD model has been imported to "ANSYS-FLUENT 16.0" to achieve the proper mesh by choosing relevant center is fine, smoothing (high), transition (fast) and span angle center (fine). The boundary conditions have been set. The total mesh nodes is equal to 34620 with 32847 cell elements as shown in figure 7. The tutbulence model (SST *k-ω*) is used to predict the recirculation zone.

The red lines as shown in figure 5 show the four locations of the test section which measures the velocity profile at upper and lower annulus flow:

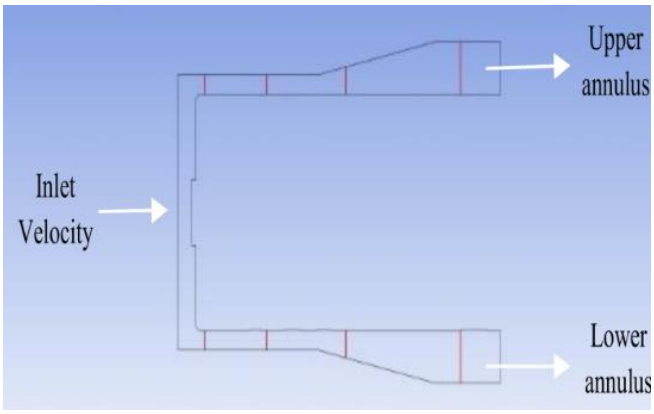

Figure 5. Display the location of four stations for upper wall casing

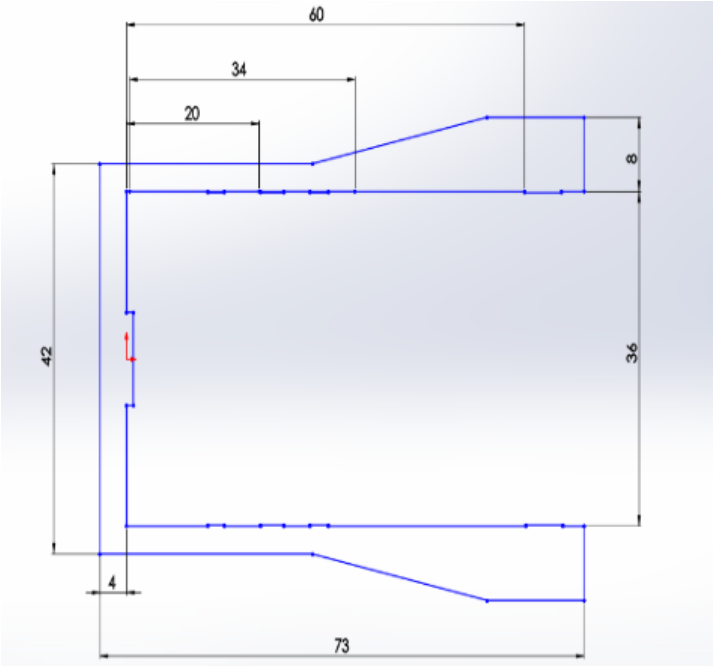

Figure 6. Schematic diagram of can combustor shows location of stations along liner wall in cm

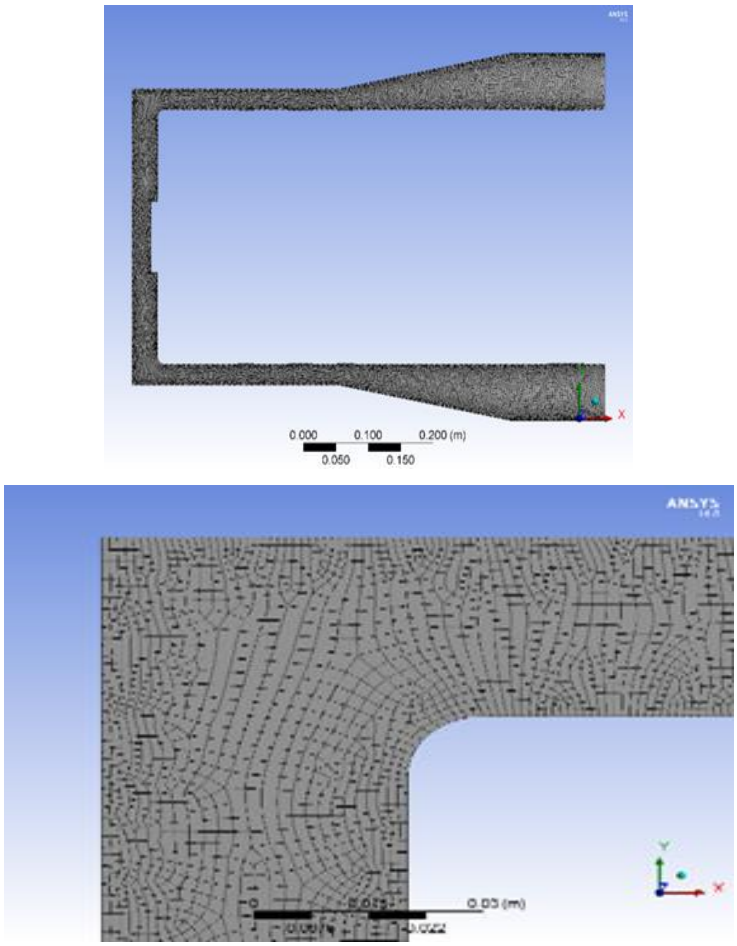

Figure 7. Shows the grid mesh

9.1. Governing equation of the mathematic model

The working fluid is assumed to be an incompressible fluid and physical parameters are constant. The governing equations that has been applied to the flow are shown in equations (4, 5 and 6) in Cartesian coordinate as follows:

Continuity equation:

$$\frac{\partial \rho}{\partial t} + \frac{\partial (\rho u_j)}{\partial x_i} = 0 \tag{4}$$

Momentum equation:

$$\rho \frac{\partial u_i}{\partial t_i} + \rho u_j \frac{\partial u_i}{\partial x_i} = - \frac{\partial p}{\partial x_i} + \mu \frac{\partial}{\partial x_j} \left(\frac{\partial u_i}{\partial x_j} + \frac{\partial u_j}{\partial x_i} \right) \quad (5)$$

Energy equation:

$$\rho \frac{\partial T}{\partial t} + \rho \frac{\partial (u_i T)}{\partial x_i} = -p \frac{\partial u_i}{\partial x_i} + \mathrm{k} \frac{\partial}{\partial x_j} \left(\frac{\partial u_i}{\partial x_j} + \frac{\partial u_j}{\partial x_i} \right) \quad (6)$$

9.2. SST k-ω models

This model is more accurate and reliable for a wider range of flows it can predict adverse pressure gradient and velocity profiles for complex geometries. The governing equations for this model are as follows:

$$\frac{\partial}{\partial t}(\rho k) + \frac{\partial}{\partial x_i}(\rho k u_i) = \frac{\partial}{\partial x_j}\left(\Gamma_k \frac{\partial k}{\partial x_j}\right) + \tilde{G}_k - Y_k + S_k \quad (7)$$

And

$$\frac{\partial}{\partial t}(\rho \omega) + \frac{\partial}{\partial x_i}(\rho \omega u_i) = \frac{\partial}{\partial x_j}\left(\Gamma_\omega \frac{\partial \omega}{\partial x_j}\right) + G_\omega - Y_\omega + D_\omega + S_\omega \quad (8)$$

Where

$$\Gamma_k = \mu + \frac{\mu_t}{\sigma_k} \quad (9)$$

$$\Gamma_\omega = \mu + \frac{\mu_t}{\sigma_\omega} \quad (10)$$

$$\mu_t = \frac{\rho k}{\omega} \frac{1}{\max[\frac{1}{\alpha^*} \frac{SF_2}{\alpha_1 \omega}]} \quad (11)$$

9.3. Boundary Condition for the wall of combustor and inlet velocity

The combustion chamber is the test section where the aerodynamic behavior inside the combustor has been simulated. The simple harmonic excitation is applied to cause a sine-wave vibrational movement. The C programing language was used to represent the sinusoidal vibrational motion. The sinusoidal vibrational velocity profile is expressed as:

$$\mathrm{V} = 2\,\pi\,{*}f\,{*}\mathrm{a}{*}\cos(2\,\pi\,\, f\,{*}\mathrm{t}) \quad (12)$$

Table 2. Boundary condition

Boundary condition	Value	
Velocity inlet	34 m/s	
Pressure Outlet	zero	
Temperature inlet	300 K	
Moving Wall	Case One	No vibration
	Case Two	80 Hz
Turbulence Intensity	5%	

10. Model validation

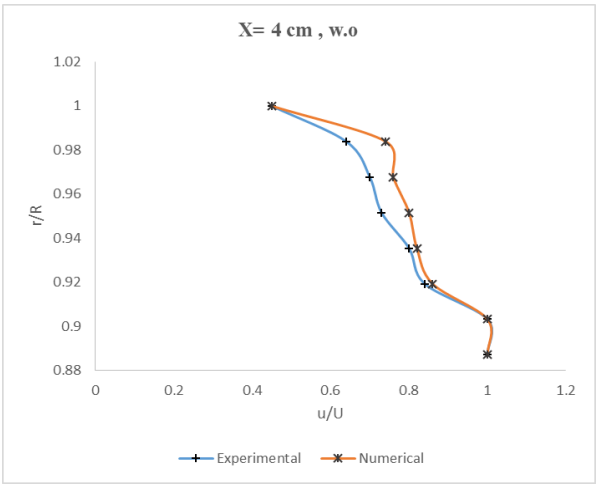

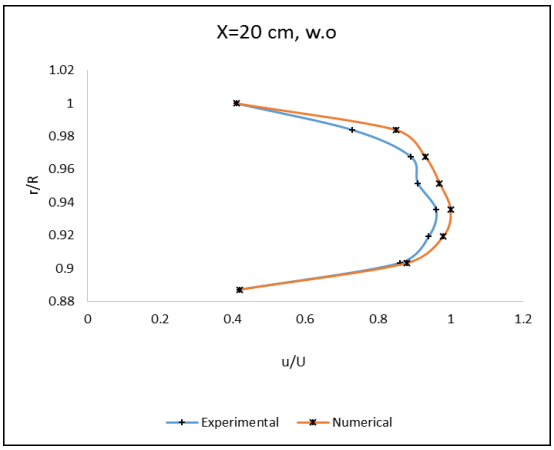

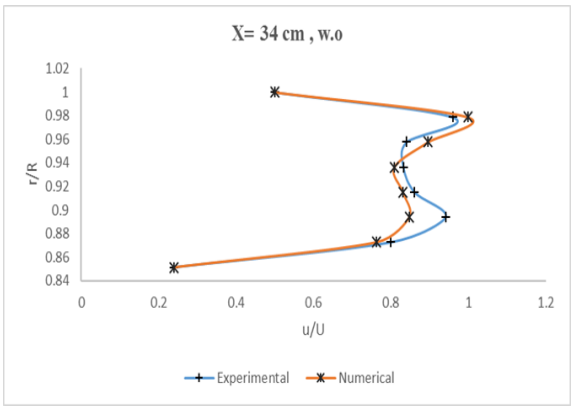

Figure 8. The velocity profile in the upper annulus with no vibration

The behavior of the annulus flow of the can combustor has been studied experimentally and numerically. A good agreement has been achieved between numerical data and experimental data. Figures 8 and 9 shows the experimental and Computational Fluid Dynamic simulation results of the velocity profile in the upper annular flow of can combustor. It was noted that at the beginning of the combustion zone, velocity profiles are not similar, because of the sharp edges of the liner head cause the disturbance of the airflow. High velocities and unstable streamlines can be identified due to the complex geometry edges. They influence on the flow stability, which will then generate a large recirculation region and reverses the flow near the liner wall of the can combustor. It can be observed that the reversed flow velocity increases with increasing frequency.

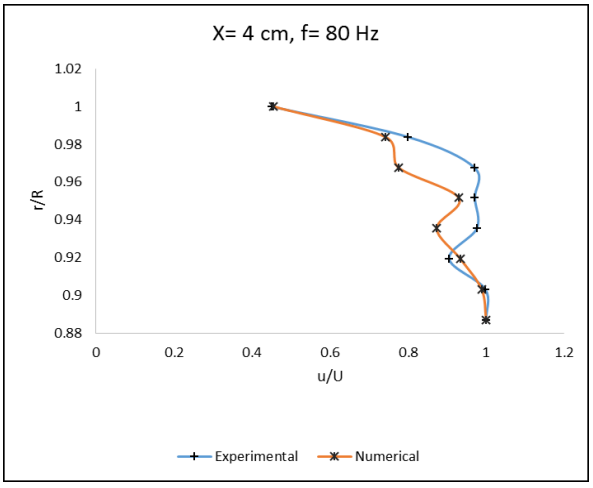

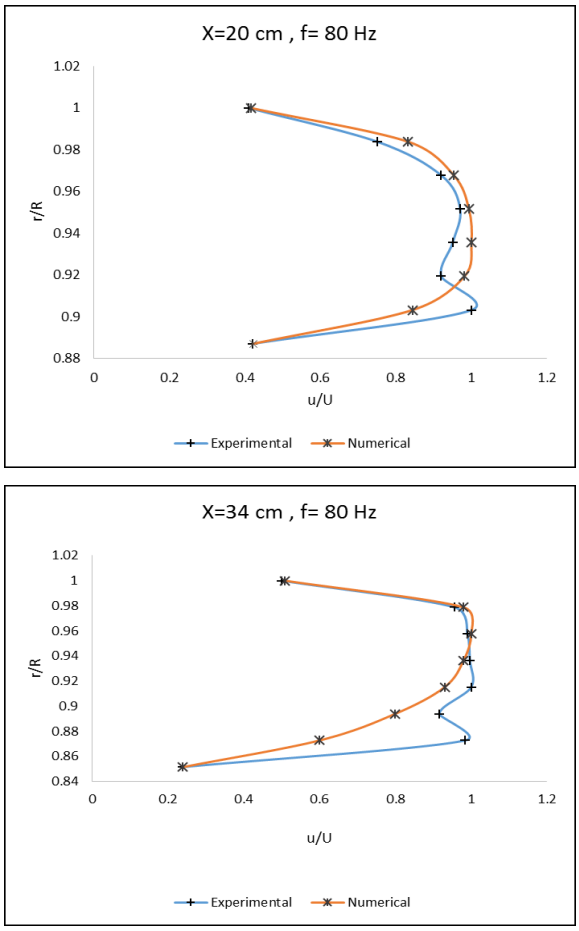

Figure 9. The velocity profile in the upper annulus at 80 Hz

11. Results and discussion

Figures 10 and 13 shows the velocity profiles for all locations. A reverse flow is noticed near the liner region of the can combustor compared with the wall of the combustor due to the dilution holes of the liner. Accordingly, the velocity at this region will be decreased as shown in the figures. Nevertheless, when the frequency increases gradually, the velocity also increases, and fluctuations of velocity increase causing the flow to be turbulence.

At the third location (X=34 cm), the velocity starts decreasing because of the cross secsional area at this position. The percentage of decrease reaches to 19% near the liner wall while the same percentage of increase will be noticed at the casing wall.

Figures 10 and 13 shows a significant reverse flow takes place especially at (r/R= 0.85-0.9) due to the instantaneous transverse velocity distribution which varies periodically and large-scale eddies are clearly identified.

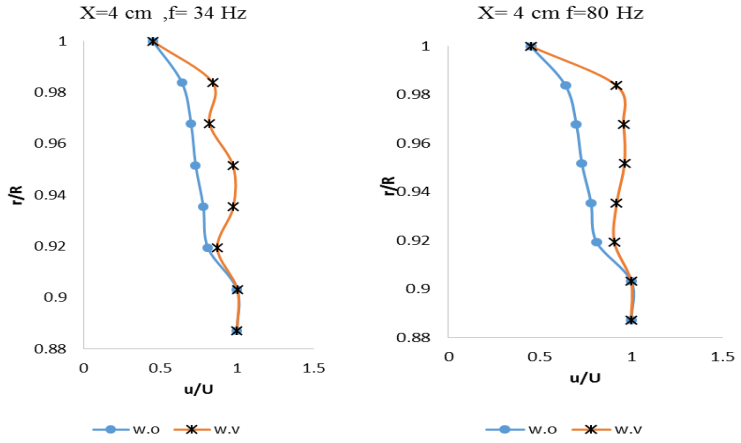

Figure 10. The velocity profile with different frequency at first station (X= 4 cm) for upper annulus

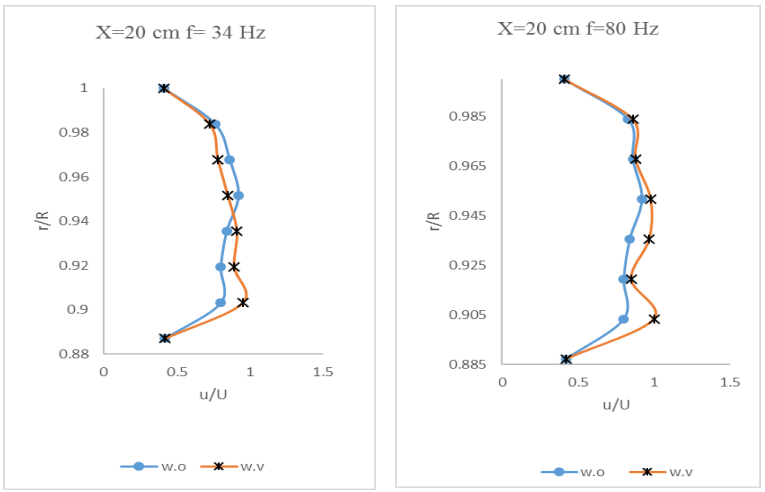

Figure 11. The velocity profile with different frequency at the second station (X=20 cm) for upper annulus

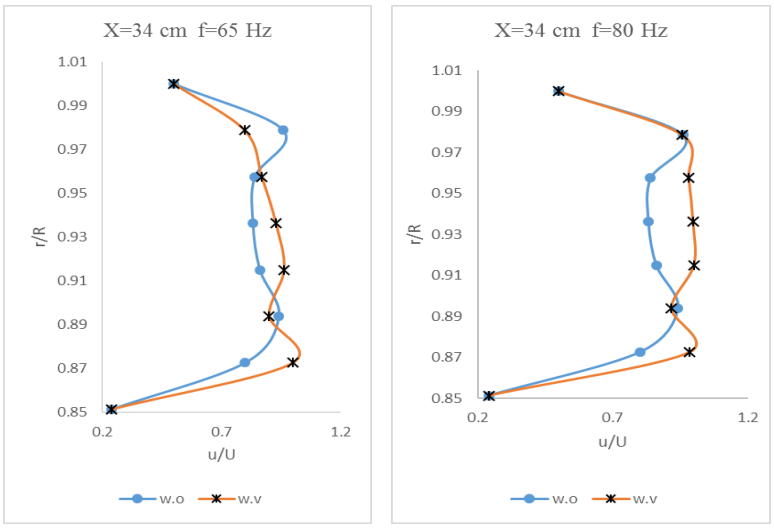

Figure 12. The velocity profile with different frequency at third station (X=34 cm) for upper annulus

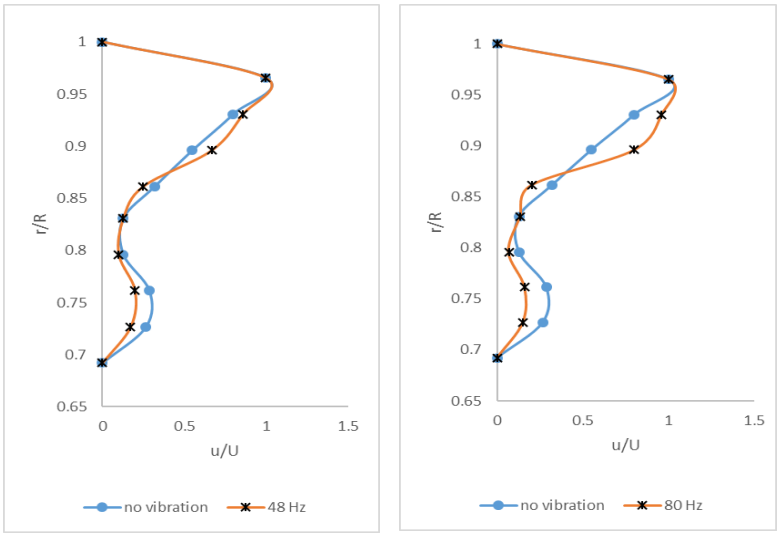

Figure 13. The velocity profile with different frequency at the fourth station (X= 60 cm) for upper annulus

The comparison between the station (X=4 cm) at the first value of forced vibration and the station (X=34 cm) when the forced vibration is maximum show that the

velocity profile increases significantly especially at the middle, because of the dynamic response of the combustor on flow velocity subjected to a single-phase flow excitation. The bigger the structural vibration, the higher the flow velocity.

It can also be seen that flow velocity increases near the liner wall of the annulus region (r/R=0.7- 0.83) at the fourth station (X=60 cm) as shown in Figure 13. The flow velocity increases when the frequency increase by (16%- 31%). The rising frequency leads to the increase of reverse flow near liner wall due to the forced vibration. However, the flow velocity increases at the center and the wall casing.

11.1. The velocity contour

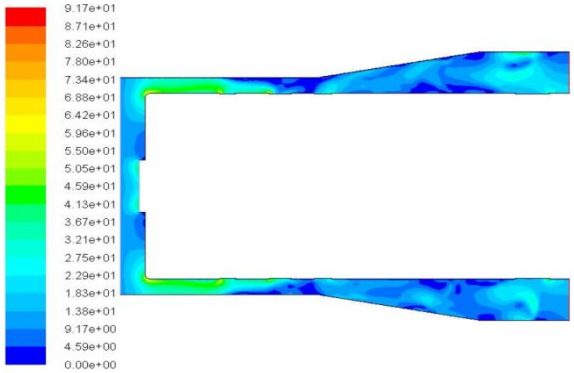

Figure 14. The contours of velocity magnitude (m/s) in Can Combustor with no vibration effect

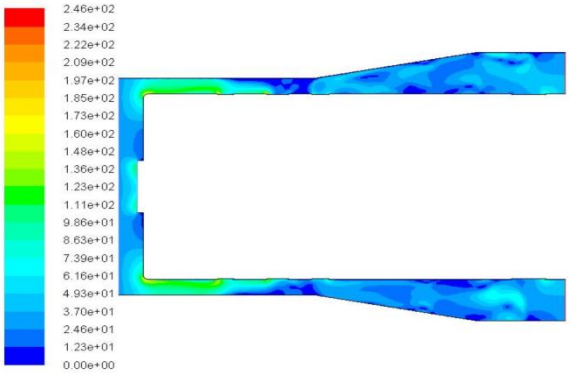

Figure 15. The contours of velocity magnitude (m/s) in Can Combustor with (80) Hz

Figure 14 shows the velocity contour magnitude for combustor without the vibration effects. At the beginning of the simulation, the values are high due to the sharp edge of the liner piece. Then, the velocity at the second station becomes higher near the casing wall but when it arrives to the dilution holes of the liner piece, the velocity magnitude decreased. At the third station, the velocity decreases due to increase of the cross-sectional area of the annulus.

In Figure 15, it can be observed that the velocity profile increased when subjected to an external load such as vibration. The combustion chamber subjected to the shaker excitation causes the flow velocities to be higher at the annulus region. The higher the vibration, the higher flow velocity.

At the inclined jet, the velocity fluctuations cause the high intensity

The fluctuating velocity values which are obtained at the inclined jet, causing the turbulence intensity to be much higher at the vibrating Combustor wall compared to a stationary case.

11.2. Turbulent intensity of annulus

In the annulus region, the turbulent flow was high and it has a great impact on velocity profile. It is considered to be the main reason which forms eddies in the annulus region of the can combustor. The turbulent intensity in annulus flow was investigated using three stations. Figures 16, 17, and 18 shows the contour of turbulent intensity for the three stations without and with the vibrational effects.

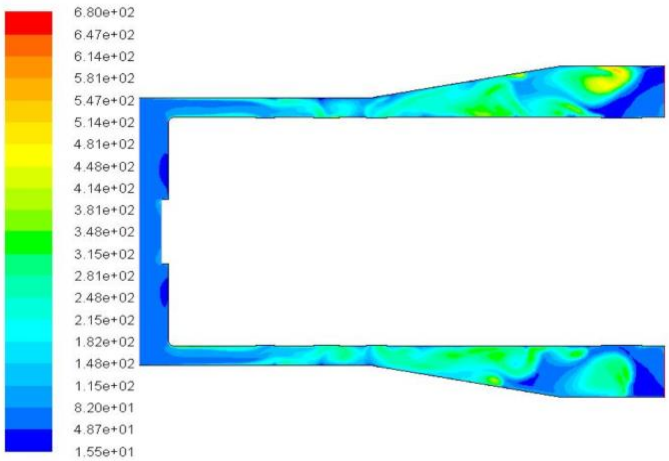

Figure 16. The Contours of turbulent intensity (%) with no vibration effect

Higher turbulence intensity zones are found near the combustor wall. The vibrating scenario, the symmetrical zones seem to have a greater turbulence intensity

at the top and bottom of the vibrating combustor and the magnitude of the turbulence intensity are clearly greater than at stationary case for the same flow velocity, this is because the combustor vibrations emerge the level velocity fluctuations, causing a significant increase in turbulence intensity of the vibrational wall combustor.

At (X= 34 cm) to the end of the annulus region (X= 60 cm), the fluctuation velocity is high which increases the turbulent intensity as shown in figure 19. At the third station (X=34 cm) with a maximum frequency (80 Hz), it is observed that the turbulent intensity profiles increased about (32%) compared with the no vibration scenario as shown in Figure 19.

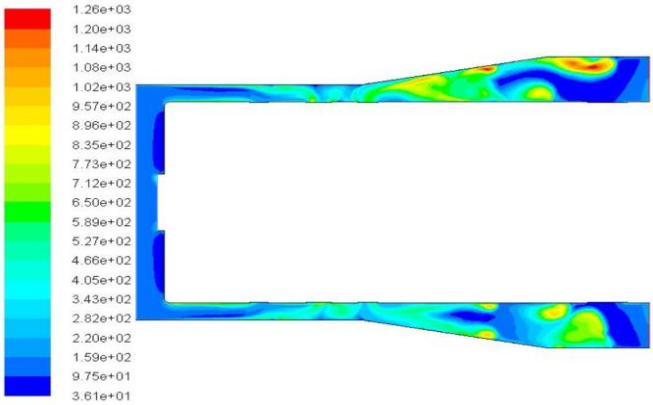

Figure 17. The contours of turbulent intensity (%) with (34 Hz) effect

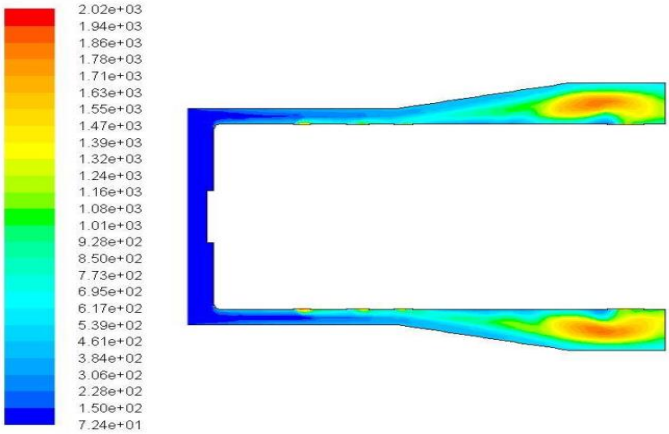

Figure 18. The contours of turbulent intensity (%) with (80 Hz) effect

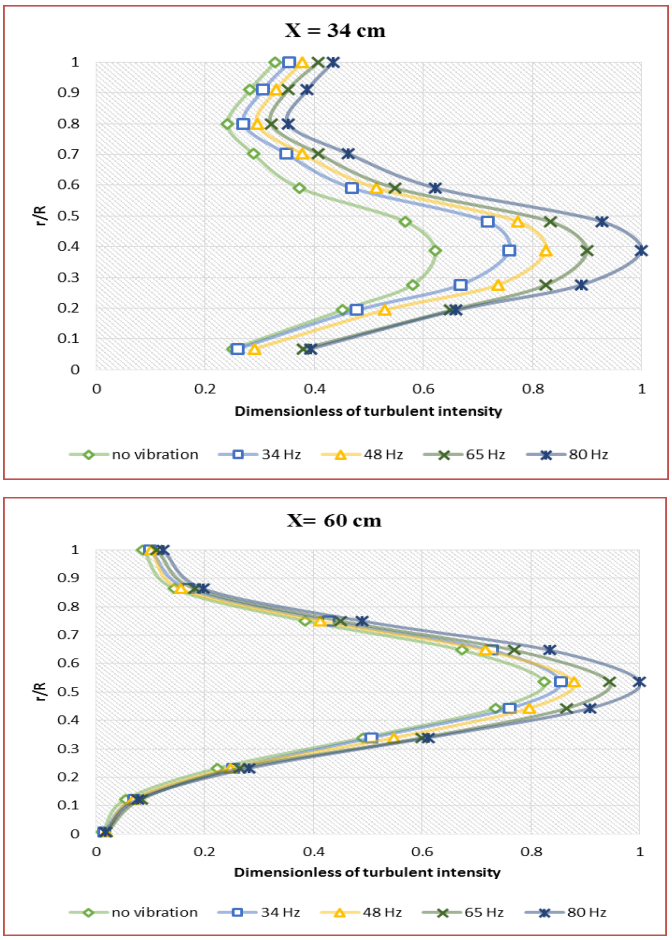

Figure 19. Turbulent intensity profile at X= 34 and 60 cm for upper annulus

12. Static pressure and pressure recovery with different frequencies

It is important to note that the annulus flow has a sufficient static pressure to achieve adequate penetration of the jets. In this study, the vibration level has negative effects on the static pressure near the liner piece and leads to reduce the air-cooling, which then reduce the lifetime of the combustor liner.

Figure 20 and figure 21 show the static pressure distribution without and with vibrational effects. In all cases at the start of the annular path, the static pressure has been decreased and then increased gradually towards the end of the combustor. The decrease occurs because of the disturbance in the flow and the generated recirculation region.

Figure 22 shows the variation of static pressure recovery coefficient at the lower annulus with and without vibration along the length of the combustor at different values of frequencies. In both scenarios, the static pressure started from positive values and decreased rapidly to the negative values. Incoming flow separated from the wall near the throat leads to a very low-pressure recovery due to the area expansion (34-60 cm), and large eddies generated form the diverging of the wall. The pressure recovery decreases due to the boundary layer thickness increase. At (X= 20, 34, 60 cm), the pressure recovery for all cases is dropped (26, 13, 7.5%) respectively due to disturbance caused by the forced vibration.

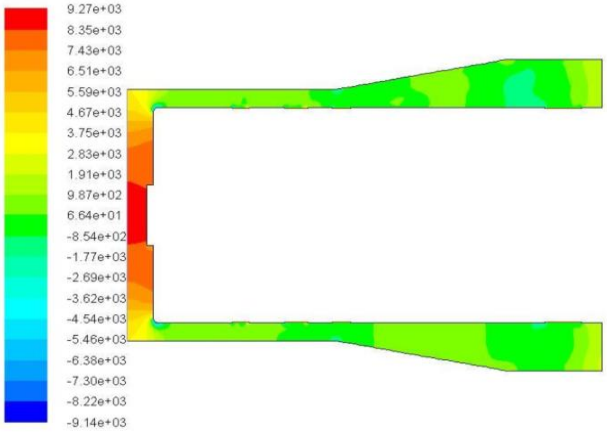

Figure 20. The contours of static pressure with no vibration effect

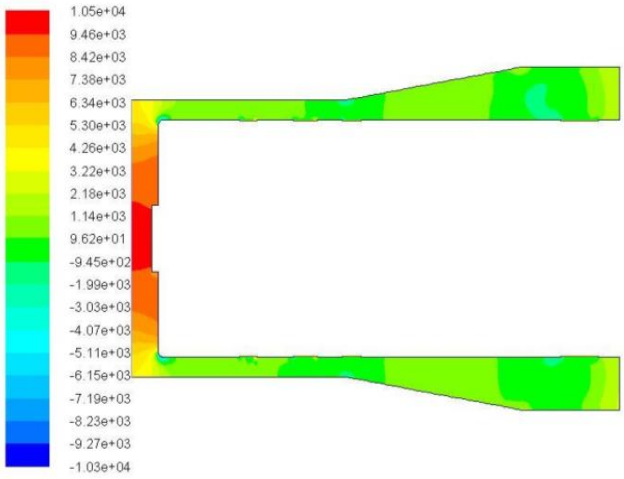

Figure 21. The contours of static pressure at 80 Hz

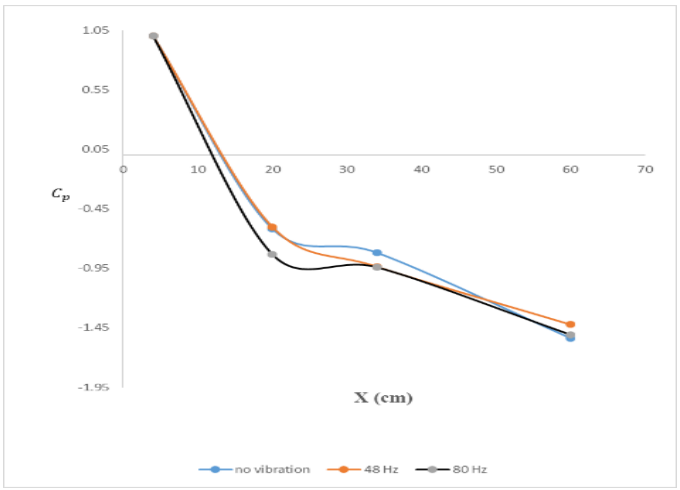

Figure 22. Shows the pressure recovery at a different frequency level

13. Conclusion

- Annulus flow characteristics for Can-Combustor are studied experimentally and numerically. Validating the Computational Fluid Dynamics results compared to the experimental results displayed a good agreement of about 94%. The SST turbulence model can be considered as a very convenient tool to inspect cold flow at annulus region with rising the frequency values.
- The investigation of the annulus flow velocity in axial direction showed that the frequency levels increase causes an increase in the velocity profile at the annulus region. Accordingly, undesirable effects will occur such as a reversible flow and large recirculation zone at particular locations.
- The airflow velocity at the location (X= 34 cm) of the liner piece with vibration is more than the velocity at the same location with no vibration senario in about (47%).
- At the location (X= 4 cm), the value of velocity profile near the wall of combustor is about (30%) more than the no vibration effect.
- The velocity profile is increased significantly especially at the core of the flow region due to the effect of the dynamic behavior of the combustor on the flow velocity subjected to a single-phase flow excitation.
- At the end of the combustor length, it can be seen that the reverse velocity becomes large due to the vibration shaker being connected directly to this particular position.

- The turbulence intensity can be affected significantly by the influence of the vibration increase, which leads to a cooling film failure.
- At the location (X= 34 cm) and in the middle point of the annulus flow, the turbulence intensity increases about (25%) when the forced vibration was applied compared to the no vibration scenario.
- The increasing flow velocity at the liner piece leads to decrease in the static pressure, which affects the performance of the cooling effectiveness, thus, the static pressure in the passage of the combustion liner should be at the highest possible level to provide a uniform flow to the combustion zones.
- Pressure recovery coefficient has been decreased with the increase of the frequency level.

Acknowledgments

This work was supported by the University of Babylon/ Mechanical Engineering department for the use of their facilities. The authors would also like to show their gratitude to the Gas Generating Station Staff for their assistance in carrying out this work.

References

Alqaraghuli W., Alkhafagiy D., Shires A. (2014). Simulation of the flow inside an annular can combustor. *International Journal of Engineering and Technology*, Vol. 3, No. 3, pp. 357-364. https://doi.org//10.14419/ijet.v3i3.2499

Al-Shorafa‟a M. H. M. (2008). A study of the influence of vertical vibration on heat transfer coefficient from horizontal cylinders. *Journal of Engineering*, pp. 14.

Cengel Y. A., Turner R. H., Cimbala J. M., Kanoglu M. (2008). Fundamentals of thermal-fluid sciences. *York: McGraw-Hill*, pp. 833-874. https://doi.org/10.1115/1.1421126

Elbaloshi A., Hu J. (2014). Simulation of Turbulent Flow in an Asymmetric Air Diffuser.

General Electrical Company operation and maintenance documentation gas turbine model (MS 9001E Frame Nine E).

Hsieh S. C., Low Y. M., Chiew Y. M. (2017). Flow characteristics around a circular cylinder undergoing vortex-induced vibration in the initial branch. *Ocean Engineering*, Vol. 129, pp. 265-278. https://doi.org//10.1016/j.oceaneng.2016.11.019

Huls R. A., Sengissen A. X., Van der Hoogt P. J. M., Kok J. B., Poinsot T., de Boer A. (2007). Vibration prediction in combustion chambers by coupling finite elements and large eddy simulations. *Journal of Sound and Vibration*, Vol. 304, No. 1, pp. 224-229. https://doi.org//10.1016/j.jsv.2007.02.027

Kwark J. H., Jeong Y. K., Jeon C. H., Chang Y. J. (2005). Effect of swirl intensity on the flow and combustion of a turbulent non-premixed flat flame. *Flow, Turbulence and Combustion*, Vol. 73, No. 3, pp. 231-257. https://doi.org//10.1007/s10494-005-4777-z

Poursaeidi E., Arablu M., Meymandi M. Y., Arhani M. M. (2013). Investigation of choking and combustion products' swirling frequency effects on gas turbine compressor blade fractures. *Journal of Fluids Engineering*, Vol. 135, No. 6, pp. 061203. https://doi.org/10.1115/1.4023852

Rahim A., Alkhafagiy D., Talukdar P. (2012). Effect of casing geometry on flow characteristics in a model can-combustor. *In ASME 2012 Gas Turbine India Conference*. *American Society of Mechanical Engineers*, pp. 73-78. https://doi.org//10.1115/GTINDIA2012-9538

Shih H. Y., Liu C. R. (2009). Combustion characteristics of a can combustor with a rotating casing for an innovative micro gas turbine. *Journal of Engineering for Gas Turbines and Power*, Vol. 131, No. 4, pp. 041501. https://doi.org/10.1115/1.3043807

Wu Y., Carlsson C., Szasz R., Peng L., Fuchs L., Bai X. S. (2016). Effect of geometrical contraction on vortex breakdown of swirling turbulent flow in a model combustor. *Fuel*, Vol. 170, pp. 210-225. https://doi.org//10.1016/j.fuel.2015.12.035

Zena K., Hadi O. (2016). Influence of vibration on free convection heat transfer from sinusoidal surface. *International Journal of Computer Applications*, Vol. 136, No. 4, pp. 1-6. https://doi.org/10.5120/ijca2016908252

Zhang D., Tan J., Lv L. (2015). Investigation of flow and mixing characteristics of supersonic mixing layer induced by forced vibration of the cantilever. *Acta Astronautica*, Vol. 117, pp. 440-449. https://doi.org/ /10.1016/j.actaastro.2015.09.001

Nomenclature

A: Area

Cp: Specific heat

D: Diameter

K: Thermal conductivity

μ: Dynamic viscosity

ρ: Density

f: frequency

P: pressure

R: Radius of combustor

Re: Reynolds Number

T: Temperature

In: Inlet velocity

Out: Outlet velocity

Exp: Experimental

Num.: Numerical

w.o: Without vibration

w.v: With vibration

H.M.I: Human Machine Interface